Proceedings of ASME Turbo Expo 2016: Turbomachinery Technical Conference and Exposition
GT2016
June 13 – 17, 2016, Seoul, South Korea

GT2016-56359

DRAFT: SPECTRA AND LARGE EDDY STRUCTURES IN THE DOUBLE LOG-LAYER OF A HIGH RE WIND TURBINE ARRAY BOUNDARY LAYER

Tanmoy Chatterjee*
Integrative Simulation & Computational Fluids Lab
Department of Mechanical & Aerospace Enegineering
SEMTE, Arizona State University
Email: tchatte3@asu.edu

Yulia Peet
Integrative Simulation & Computational Fluids Lab
Department of Mechanical & Aerospace Enegineering
SEMTE, Arizona State University
Email: ypeet@asu.edu

ABSTRACT

Wind Turbine Array Boundary Layer (WTABL) is a relatively simple, yet useful theoretical conceptualization to study very large wind farms in atmospheric boundary layer (ABL). In the current paper, we perform a high-fidelity LES investigation of a 3 × 3 wind turbine array in a WTABL framework, with a main focus on extending the work beyond the simple analytical model and providing a rigorous fundamental understanding of the dynamic behaviour of length scales, their scaling laws and the anisotropic structure of the energy containing eddies responsible for power generation from the wind turbines. This is accomplished by studying the components of energy and shear-stress spectra in the flow. This knowledge can potentially provide an efficient way to control the wind farm power output as well as serve as a stepping stone to design efficient low order numerical models for predicting farm power and dynamics at reduced computational expense.

NOMENCLATURE

x, y, z Streamwise, spanwise and wall normal direction
u, v, w Streamwise, spanwise and wall normal velocity
$\widetilde{\mathbf{u}}_h$ Filtered horizonal velocity vector
$\boldsymbol{\tau}_s$ horizontal shear stress vector at bottom wall
U Temporally averaged streamwise velocity
$\langle\rangle$ Horizontal averaging in xy plane
l_f Filter length scale of Smagorinsky model
ν_t Eddy viscosity
Δz Distance of first GLL grid point from the wall
C_l, C_d Lift and Drag coefficient
c, w_d Chord length and width of the turbine blades
α Angle of attack
γ Pitch angle
V_{rel} Relative velocity of fluid in the blade frame
k_x, k_y Streamwise, spanwise wavenumber
λ_x, λ_y streamwise, spanwise wavelength normalized by H
H Atmospheric boundary layer thickness
u_* Friction velocity scale of ABL
$u_{*,lo}, u_{*,hi}$ Friction velocity scale below and above z_h
z_0 Aerodynamic roughness for ABL
$z_{0,lo}$, $z_{0,hi}$ Aerodynamic roughness below and above z_h
κ Von Karman Constant
D Wind turbine rotor diameter
z_h Hub height of the wind turbines
U_{hub} Temporally averaged streamwise velocity at hub height z_h
E_{uu}, E_{vv}, E_{ww}, ϕ_{uw} streamwise, spanwise, wall normal energy spectra, & cospectra

INTRODUCTION

Since the mid-1980's, wind energy has begun to evolve into one of the rapidly emerging and developing fields of research as a cleaner alternative to fossil and nuclear fuels. Large wind farms comprising of many arrays of wind turbines are deployed to harvest wind power from the atmospheric boundary layer (ABL). In

*Address all correspondence to this author.

the numerical framework, the problem is extremely complex, because of the large scale separation induced by (a) geometry of the farms (the streamwise extent is usually much larger than 10 times the boundary layer thickness) [1, 2] as well as by the (b) high Reynolds number ($Re = 10^{10}$) of the atmospheric flows [3]. The scale separation induced by the geometry of the wind farm can be simplified by using the model of "Wind Turbine Array Boundary Layer" (WTABL) [2] which ensures that the growth of the inner layer due to wind turbine wake expansion is saturated and hence shorter periodic domains can be employed. Also, the wide range of scale separation in wall-wake turbulence induced by the high Reynolds number flow renders Direct Numerical Simulations (DNS) to be cost-prohibitive ($N_x \times N_y \times N_z \sim O(Re^{2.7})$) [4]) and hence we capture the dynamically important, large-scale structures in the flow (major contributors to wind turbine power) using Large Eddy Simulation(LES) [2,5].

Fully developed WTABL is in many ways comparable to the rough wall neutral ABL model, however it features the presence of *two equilibrium layers*, both satisfying the log law of the wall and the streamwise-spanwise homogeneity in the computational domain. For WTABL, simple **equilibrium solutions** exist; (a) *balance between pressure gradient and turbulent dissipation work* and (b) *balance between body force work (a fraction of which is converted to wind power) and turbulent shear stress flux difference*. The analytical model by Frandsen et al. [1] which was later extended by Calaf et al. [2] has been so far successful in describing the power generated by a wind turbine array by the downward vertical entrainment of turbulent flux. However, despite the progress of turbulent wind wake model for industrial purpose, much less is known about the **physics and length-scale of the eddies** that contain substantial kinetic energy and shear stress intercepting the turbine that imparts a major contribution on the power generated by them. Studies regarding eddies or "coherent structures" and their lengthscales at high *Re* flows have gained momentum since the 1970's along the lines of *Attached Eddy Hypothesis*. It was established that these eddies make up the log-layer and considerable amount of turbulence production [6, 7]. This theory has revived renewed interest with the discovery of Large and Very Large Scale Motions (LSM's and VLSM's) [8] which contain a significant fraction of the kinetic energy. However, the fundamental studies of large scale eddies (LSE) even though quite popular among canonical wall-bounded flows have not been performed in the area of wind turbine aerodynamics except for some recent attempts by Hamilton et al. [9] to analyse the LSE involved in the power generation. Figure 3 shows an example of large-scale structures ($\sim O(H)$) present in wind farms (current computations).

In the current paper we perform an LES with near wall modelling of a 3×3 wind turbine array in a neutral ABL ($Re = 10^{10}$), with a computational domain similar to the experimental set up of [9, 10]. The wind turbines are modelled using the state-of-art Actuator Line (AL) method [11] without having to resolve the wind turbine blades. The statistical results are benchmarked against the analytical model of Frandsen as well as the previous literature [1, 2].

The main objective of the paper lies in performing a detailed analysis of the LSE in the inner and outer layer of ABL, some of which play an important role in turbine power generation, with the help of metrics like 1D, 2D energy and shear-stress spectra (against streamwise and / or spanwise wavelengths). This paper addresses some of the fundamental questions/problems given below regarding the eddy structures and their dynamic behaviour that have not been or have only partially been addressed (as in (a)) in the previous literature. (a) *What is the most dominant length scale and structure of the eddies that contribute to the power generation?* (b) *How is the attached eddy layer structure and their length scales affected with the "wind turbine roughness" being imposed in the neutral ABL?* (c) *How can the dynamical behaviour of eddies in the double log-layer and the wake mixing layer in the rotor-swept area be represented, possibly with some scaling laws ?* The inquiry addressed in the current paper not only helps develop a strong rudimentary background of the wind farm dynamics but also provides a potential to use the above information to control the power-efficiency of the wind-farm.

NUMERICAL METHOD

The numerical method implements a variational formulation of Navier-Stokes equation involving Galerkin projection using open-source spectral element solver **Nek5000** [12]. The domain is partitioned into hexahedral elements in 3D, and within each element any variable can be expanded into a series of orthogonal basis functions (Lagrange-Legendre polynomials) with the grid points clustered towards the element boundaries known as Gauss-Lobato-Legendre (GLL) points which are essentially the roots of the basis function polynomials. For smooth solutions, exponential convergence can be achieved with increasing order of the polynomials.

The time discretization of NS solver in Nek5000 involves third order backward difference scheme, the velocity is solved using preconditioned conjugate gradient (CG) method and the pressure solver uses iterative generalized mean residual solver (GMRES) method in Krylov subspace. The current algorithm was optimized to achieve perfect scalability in parallel implementation up to 1,000,000 processors [12].

GOVERNING EQUATIONS AND LARGE EDDY SIMULATION

The spatially filtered 3D Navier-Stokes equation for LES of wind turbine arrays in neutral ABL flows can be obtained by incorporating a convolution integral filter on the original Navier-Stokes

equation

$$\frac{\partial \widetilde{\mathbf{u}}}{\partial t} + \widetilde{\mathbf{u}}\nabla\widetilde{\mathbf{u}} + \frac{1}{\rho}\nabla\widetilde{p^*} - \widetilde{\mathbf{F}} - \nu\nabla^2\widetilde{\mathbf{u}} = -\nabla\cdot\boldsymbol{\tau}(\mathbf{u},\mathbf{u}) \qquad (1)$$

The subgrid stress (SGS) tensor in Equation 1, $\boldsymbol{\tau}(\mathbf{u},\mathbf{u}) = \widetilde{\mathbf{u}\mathbf{u}^T} - \widetilde{\mathbf{u}}\widetilde{\mathbf{u}}^T$ arising from the non-commutativity of filtering with the nonlinear advection term, is modelled using a Smagorinsky type eddy viscosity closure. The model SGS stress $\boldsymbol{\tau}^{SGS}(\widetilde{\mathbf{u}},\widetilde{\mathbf{u}})$ can be given as $\boldsymbol{\tau}^{SGS} - \frac{1}{3}tr(\boldsymbol{\tau}^{SGS})\mathbb{I} = -2\nu_t\nabla^s\widetilde{\mathbf{u}}$. In classical Smagorinsky model, $\nu_t = (l_f)^2|\nabla^s\widetilde{\mathbf{u}}|$, with $l_f = C_s\Delta$ [13], Δ is a grid scale and the term $|\nabla^s\widetilde{\mathbf{u}}|$ can be given as $|\nabla^s\widetilde{\mathbf{u}}|^2 = 2\nabla^s\widetilde{\mathbf{u}} : \nabla^s\widetilde{\mathbf{u}}$ and $\nabla^s\widetilde{\mathbf{u}} = \frac{1}{2}(\nabla\widetilde{\mathbf{u}} + \nabla\widetilde{\mathbf{u}}^T)$. For high Reynolds number turbulent ABL flow, we employ the algebraic wall damping by Mason and Thompson (1992) [13],

$$\frac{1}{l_f^n} = \frac{1}{(C_0\Delta)^n} + \frac{1}{\kappa(z+z_0)^n} \quad z_0 \ll H. \qquad (2)$$

For best results in our SEM model (see [14] for details), the ad-hoc blending function parameters $C_0 = 0.19,\ n = 0.5$ are used.

Model assumptions: Boundary conditions and Near Wall Modelling

We incorporate periodic boundary conditions in the streamwise and spanwise direction while the top boundary conditions are stress free. At the bottom surface, we use a wall stress boundary condition without having to resolve the rough wall, relating the wall stress vector to the horizontal velocity vector $\widetilde{\boldsymbol{u}}_h$ at the first grid-point using the standard Monin-Obukhov similarity law [15] along with no-penetration conditions of large eddies, $\widetilde{w} = 0$.

$$\frac{1}{\rho}\boldsymbol{\tau}_s = -\kappa^2 \frac{\widehat{\widetilde{\boldsymbol{u}}}_{h,\frac{\Delta z}{2}}(x,y,t)\,|\,\widehat{\widetilde{\boldsymbol{u}}}_{h,\frac{\Delta z}{2}}|(x,y,t)}{\log(\frac{z}{z_0})\Big|^2_{\frac{\Delta z}{2}}} \qquad (3)$$

where, $|\,\widehat{\widetilde{\boldsymbol{u}}}_{h,\frac{\Delta z}{2}}| = \sqrt{\widehat{\widetilde{u}}^2_{\frac{\Delta z}{2}} + \widehat{\widetilde{v}}^2_{\frac{\Delta z}{2}}}$ and $\widehat{\widetilde{\boldsymbol{u}}}_{h,\frac{\Delta z}{2}} = \widehat{\widetilde{u}}_{\frac{\Delta z}{2}}\vec{e}_x + \widehat{\widetilde{v}}_{\frac{\Delta z}{2}}\vec{e}_y$ ($\vec{e}_x, \vec{e}_y$ are unit vectors in the x,y direction). The "hat" represents additional explicit filtering carried out in the modal space by attenuating $k_c = 4$, highest Legendre polynomial modes of the spectral element model [14]. For collocated spectral element methods $\widehat{\widetilde{u}}_{\frac{\Delta z}{2}}, \widehat{\widetilde{v}}_{\frac{\Delta z}{2}}$ are calculated as an interpolation at half wall node $\Delta z/2$ e.g., between $\widehat{\widetilde{u}}(x,y,0,t)$ and $\widehat{\widetilde{u}}(x,y,z=\Delta z,t)$ (and similar procedure for $\widehat{\widetilde{v}}$) and $\Delta z/z_0 \gg 1$.

ACTUATOR LINE MODEL

In an actuator line model [16], the blades of aerofoil cross section are divided into elements, similar to the Blade Element Momentum Theory (BEM), and the local lift (L) and drag (D) force experienced by each element is calculated as $(L\ ,\ D) = \frac{1}{2}C_{(l,d)}(\alpha)\,\rho\,V^2_{rel}\,c\,w_d$ and C_l, C_d of the aerofoil are computed beforehand from DNS or wind-tunnel experiments. In the current paper, C_l, C_d were taken from standard NACA airfoil look-up tables, no 3D or stall corrections were implemented. The local aerodynamic force $\vec{f} = L\vec{e}_L + D\vec{e}_D$ (here $\vec{e}_L$ and $\vec{e}_D$ are the unit vectors in the direction of the local lift and drag, respectively) can be calculated by computing α from V_{rel}, streamwise velocity V_x and γ (Figure 1). The total reaction force from all the blade elements experienced by the fluid distributed smoothly on several mesh points is given by

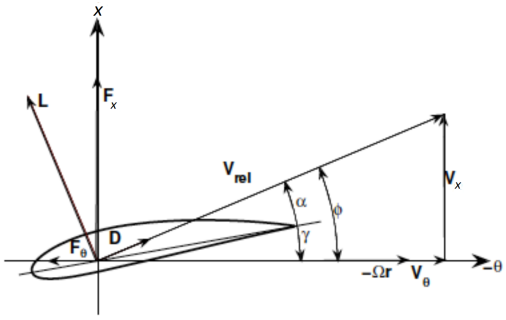

FIGURE 1: VELOCITY TRIANGLE FOR THE DETERMINATION OF THE LOCAL RELATIVE VELOCITY ON A TURBINE BLADE.

$$\vec{F}(x,y,z,t) = -\sum_{i=1}^{N}\vec{f}(x_i,y_i,z_i,t)\,\eta_\varepsilon(|\vec{r}-\vec{r}_i|), \qquad (4)$$

using a smeared out delta function in the form of a Gaussian $\eta_\varepsilon(d) = 1/\varepsilon^3\pi^{3/2}\exp\left[-\left(d/\varepsilon\right)^2\right]$. The summation in the forces is over all N blade elements, and $\varepsilon = 2\,w_d$ is used in the current study for optimum results. The AL model is more advanced than the actuator-disc model [2] commonly used in numerical computations of WTABL, in its capability to capture the tip-vortices being shed in the near-wake quite accurately [14, 16].

HORIZONTALLY AVERAGED WTABL: VALIDATION OF ANALYTICAL MODEL

The periodic computational domain for studying Wind Turbine (WT) array is $21D \times 9D \times 3D$ (See Figure 2(a)), containing a 3×3 array of 3 bladed wind turbines spaced s_xD and s_yD apart in the streamwise and spanwise direction ($s_x = 7, s_y = 3$) and wind turbine hub height at $z_h = D$. For comparison purpose, a simulation with neutral atmospheric boundary layer has also been computed in a similar domain without the wind turbine arrays. The Reynolds number based on BL thickness H for both

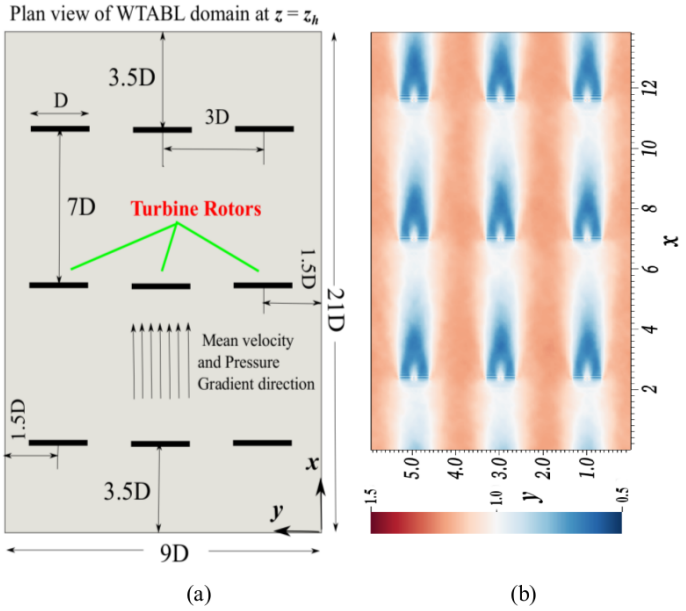

FIGURE 2: (A) PLAN (xy PLANE) VIEW OF THE COMPUTATIONAL DOMAIN OF WIND TURBINE ARRAY. (B) TEMPORAL AVERAGE OF NORMALIZED STREAMWISE VELOCITY U/U_{hub} AT xy PLANE, $z = z_h$

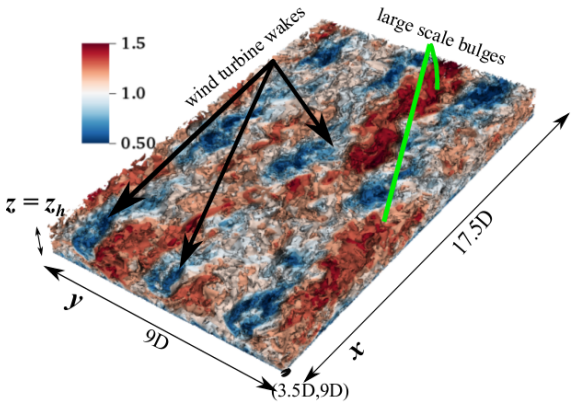

FIGURE 3: ISOSURFACE OF NORMALIZED VELOCITY MAGNITUDE $\sqrt{u^2+v^2+w^2}/U_{hub}$ IN WIND TURBINE ARRAY

the computations is $Re = 10^{10}$ and $D = 0.33H$. For details of the turbine parameters, refer to [14]. The number of elements in the WT array simulation is $42 \times 30 \times 24$ (~ 20 million grid points), while for ABL simulation it is slightly lower, $30 \times 20 \times 24$ (~ 5 million grid points) with 7^{th} order Lagrange-Legendre polynomial as SEM basis function for both the geometries. Roughly 30 grids points are used in the rotor-swept region of yz plane of WT domain for resolving the wind turbine wakes. Apart from validating the "*exponential convergence*" of grids with GLL points, grids for both the geometry were designed in the **High-Accuracy zone** (HAZ) along the lines of Brasseur and Wei [17] eliminating the over-disspative effects of the LES model.

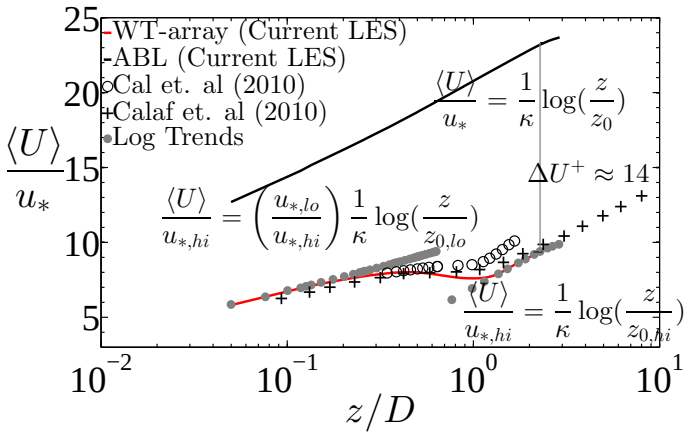

FIGURE 4: DOUBLE LOGARITHMIC TRENDS OF MEAN-STREAMWISE VELOCITY IN WTABL ABOVE AND BELOW THE WIND TURBINES. FOR ABL FLOWS, $u_{*,hi} = u_{*,lo} = u_*$. THE MAIN WTABL VELOCITY PLOTS IS NORMALIZED BY $u_{*,hi}$. $z_0 = z_{0,lo} = 10^{-4}H$. ΔU^+ IS THE HAMMA ROUGHNESS FUNCTION.

Although, the number of turbines and the size of the domain may be slightly smaller than in similar studies [2], the use of periodic boundary conditions in the horizontal plane to enforce directional homogeneity and very long simulation time (30 eddy turn over times, $H/u_{*,hi}$) ensures that the computational setup can be considered effectively fully developed.

The current computations in WTABL regime have been benchmarked against the experimental results of Cal et al. [10] as shown in Figure 4, 5. Figure 4 shows excellent trends of double logarithmic equilibrium layer [1, 2, 10]) of the mean streamwise velocity $\langle U \rangle$ predicted from current simulations. Analysis of the two equilibrium layers suggest, that the lower logarithmic layer ($z < z_h$) characterized by $u_{*,lo}, z_{0,lo} = z_0$ is due to the bottom wall roughness, the top logarithmic trend ($z > z_h$) characterized by $u_{*,hi}, z_{0,hi} > z_0$ is due to the roughness imposed by "wind turbine array", while the transition region between the log trends is a perfectly mixed layer due to turbulent wake dissipation [2] in the rotor-swept area. The Hamma roughness function $\Delta U^+ = 1/\kappa \log\left(z_{0,hi}/z_{0,lo}\right)$, depicting a downward shift of the logarithmic intercept of WT array compared to ABL provides a quantitative estimate of the turbine array roughness $z_{0,hi}$. In WTABL, in addition to the Reynolds stresses $\langle \overline{u'w'} \rangle$, the dispersive or the canopy stresses $\langle \tilde{u}''\tilde{w}'' \rangle$ [2, 10] and their fluxes also play a significant role in turbulence production (dispersive stresses are absent in neutral ABL flows), arising due the corre-

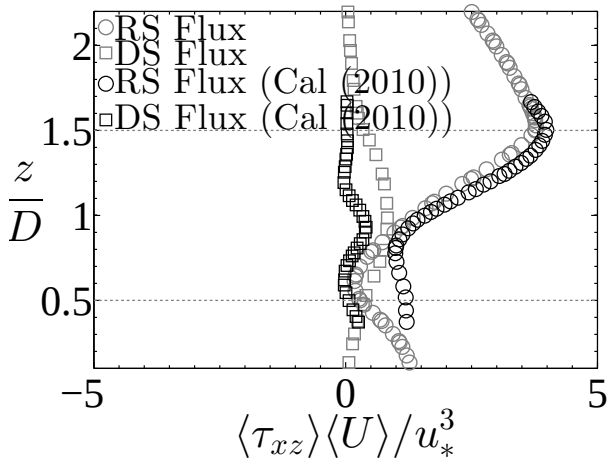

FIGURE 5: TEMPORALLY AND PLANAR (xy) AVERAGED TURBULENT SHEAR STRESS FLUXES WITH WIND TURBINE ARRAYS. CONTRIBUTION FROM THE STREAMWISE FLUXES OF REYNOLDS STRESSES (RS), DISPERSIVE STRESSES (DS) FROM CURRENT LES ARE COMPARED AGAINST CAL ET AL. (2010) [4]. DASHED LINES: ROTOR SWEPT AREA BETWEEN $z_h - D/2$ & $z_h + D/2$

lations between the spatially non-homogeneous mean horizontal and mean vertical velocities. The results from the current simulation (Figure 5) corroborates the analytical model [1, 2] which shows that the power extracted from the wind turbine comes mainly from the **downward vertical entrainment** of the mean kinetic energy as shown in the difference of mean kinetic energy flux at $z_h \pm D/2$ through turbulent shear stresses ($-\langle\overline{u'w'}\rangle\langle U\rangle$, $-\langle\bar{u}''\bar{w}''\rangle\langle U\rangle$). The difference between the shear stress flux (reynolds + dispersive) at $z_h \pm D/2 \sim 0.40$ is the same order of magnitude as the power coefficient $C_p \sim 0.25$ by each wind turbines as validated from the previous literature [2, 9, 10]. However, despite the simplified equilibrium laws in WTABL models [1, 2], they lack the essential details of the dynamic behaviour of dominant length scales needed to answer the questions in the introduction. These length scales are obtained in the present paper from the analysis of important turbulence metrics like kinetic energy, shear stress in wavenumber space (k_x, k_y) by invoking Fourier transform, with the definition of these length scales or wavelengths being $\lambda_{x,y} \sim 2\pi/k_{x,y}$. All spectra presented below have been temporally averaged.

ENERGY SPECTRA AND COSPECTRA

1D Spectra

In the current section we present the plots of 1D energy and shear-stress spectra (normalized by $u_\tau^2 z$) vs normalized streamwise wavenumber $k_x z$ with and without the wind turbine arrays (Figures 6, 7). As seen in the previous literatures, Townsend-Perry attached eddy hypothesis [6, 7] serves as a robust building block in understanding the behaviour of near-wall eddies of canonical wall-bounded flows. The signatures of the energy spectra and cospectra for the attached eddies in Figure 6 have been obtained for the neutral ABL and are well validated against the previous literature. In high Re neutral ABL flows, two distinct "*overlap*" regions exist in the variation of u, v energy spectra (Figures 6a, 6c) as manifested by the k_x^{-1} (overlap between integral and inertial scales) and the $k_x^{-5/3}$ law (overlap between inertial and Kolomogorov scale), while the w energy spectra in Figure 7a, has only one overlap region illustrated by the $k_x^{-5/3}$ law in the outer layer. Likewise the shear stress cospectra in Figure 7c also recovers a $k_x^{-7/3}$ law [9] at the extreme outer region. The regions of $k_x^{-1/2}$ and $k_x^{-5/3}$ laws come from the large-intermediate scales in the attached layer in the near-wall due to the highly-correlated u, w regions, $\phi_{uw}(k_x, z) \approx E_{uu}(k_x, z)^{1/2} E_{ww}(k_x, z)^{1/2}$.

These scaling laws as described above are also pesent with the WT arrays but decreases the extent ($k_x z$ span) of it as seen in the u, v, w and $-\overline{u'w'}$ spectra (See Figures 6b, 6d, 7b, 7d) Additionally, conspicuous peaks at hub-height ($z/H = 0.33$) in the energy and shear-stress spectra can be seen at $k_x z \sim O(10^1 - 10^2)$ with the **dominant peak** occurring in the w spectra in Figure 7b, followed by uw cospectra (Figure 7d), u (Figure 6b) and lastly v (Figure 6d). Moreover, in WT arrays the tails of the spectra ($k_x z > 10^1$) display a prominent difference at $z/H = 0.1667, 0.5, 0.875$ (at the rotor-swept region $z = z_h \pm D/2$ and further outer layer) compared against the neutral ABL in terms of delaying the dissipative decay of the spectra towards larger wavenumbers. This **delay** at the spectral tails can be largely attributed due to the "energy / stress injection" mechanisms (much smoother than at hub-height $z/H = 0.333$) corresponding to a span of scales at $k_x z \sim O(10^1 - 10^2)$. Consequently, the streamwise length-scales λ_x responsible for the "energy injection" at hub-height can be calculated as $\lambda_x \sim 0.05082H$ or $\lambda_x \approx 0.15D$ corresponding to the maximum peak-location of the spectra of WT-arrays (Figures 6b, 6d, 7b, 7d) while the delay in spectral tails, probably due to the indirect effects of energy injection occurs at length scales $\lambda_x \sim 0.02H - 0.2H$ or $0.06D - 0.6D$. Larger length scales $\lambda_x \approx 2H = 6D$ corresponding to $k_x z \sim O(10^0)$ also have their effects of "energy injection" as discernibly observed in the smoother peaks of u and $-\overline{u'w'}$ spectra.

Unless otherwise mentioned, for all plots of 1D spectra, $u_\tau = u_*$ for neutral ABL and $u_\tau = u_{*,hi}$ for WT arrays. All the normalized spectral curve should collapse into a single curve for neutral ABL, with a change of slope at $k_x z \sim O(1)$. However, the collapse of the normalized spectra in WT array is less prominent compared to ABL, possibly due the absence of a *unique friction velocity scale*. Furthermore, even though the WT array has two distinct length scales D and H, all our spectral analysis use only H for meaningful comparison with ABL and D can be interpreted

as a fraction of H.

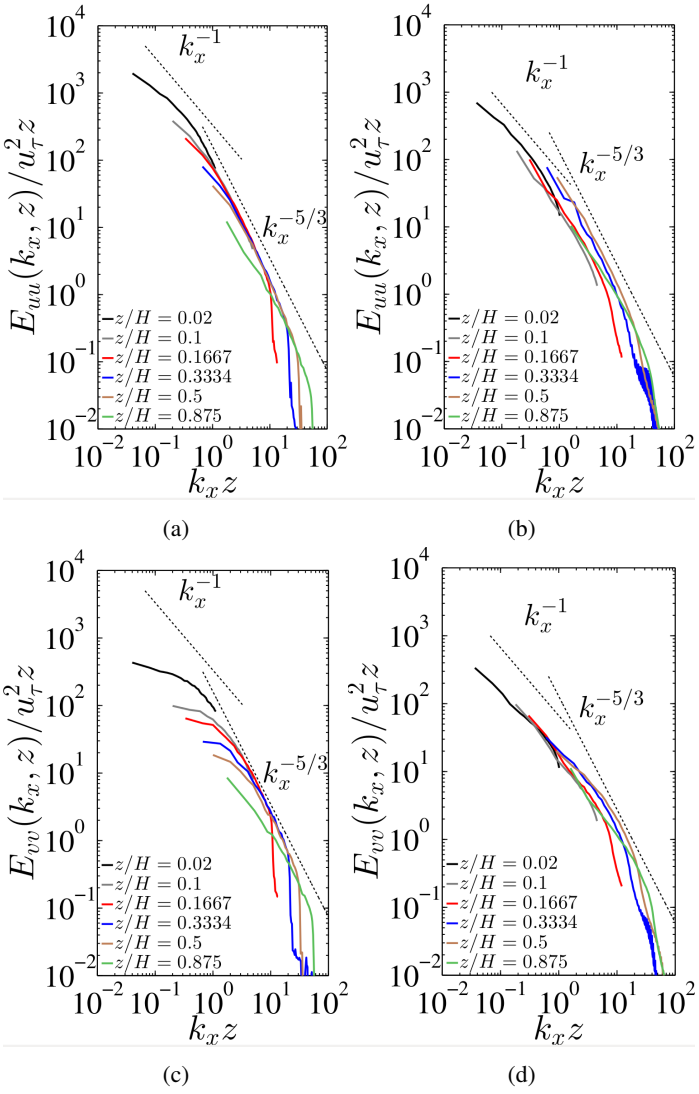

FIGURE 6: COMPARISON OF SPANWISE AVERAGED 1D u,v ENERGY SPECTRA VS NORMALIZED WAVENUMBER $k_x z$ BETWEEN, LEFT: WITHOUT WIND TURBINES, RIGHT: WITH WIND TURBINES

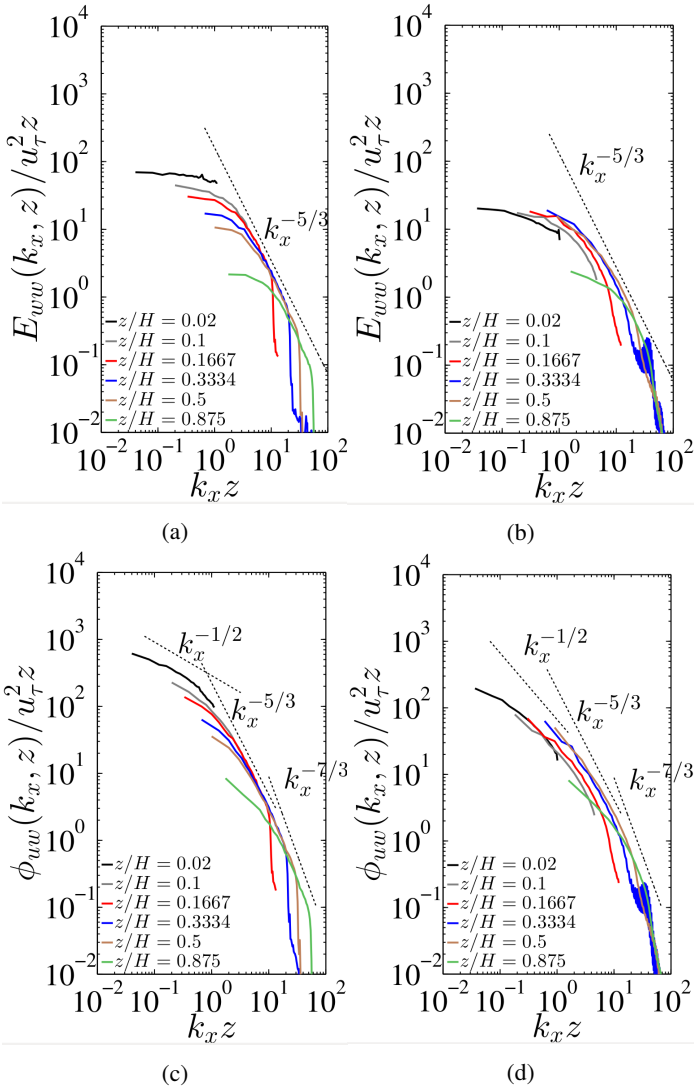

FIGURE 7: COMPARISON OF SPANWISE AVERAGED 1D w ENERGY SPECTRA AND SHEAR STRESS $-\overline{u'w'}$ COSPECTRA VS NORMALIZED WAVENUMBER $k_x z$ BETWEEN, LEFT: WITHOUT WIND TURBINES, RIGHT: WITH WIND TURBINES

2D premultiplied Spectra

While the 1D spectra provides an estimate of the length scales of the eddies responsible for the "energy injection" in the flow, its 2D counterpart complements the analysis by elucidating on the structure of the eddies and the degree of their anisotropy. It must be mentioned that in a statistically stationary flow like WTABL, we can seek an **equilibrium** between the "energy injection" in the flow and "energy generation" by the turbines at *large length scales* where linear mechanisms are dominant. In particular, the 2D filtered premultiplied energy and shear stress spectra (e.g. $k_x k_y E_{uu}(k_x,k_y)$ for streamwise spectra) in the streamwise-spanwise wavenumber plane at different z levels, (contour level 0.125 of maximum; additionally 0.05 of maximum shown for WT arrays for $z/H > 0.3$) are shown in Figures 8, 9, 10, 11. All the spectra are normalized with u_τ^2. In the past, [18–20] has made a successful use of the 2D energy and shear-stress spectra for capturing the size of the "turbulent objects" that constitute the

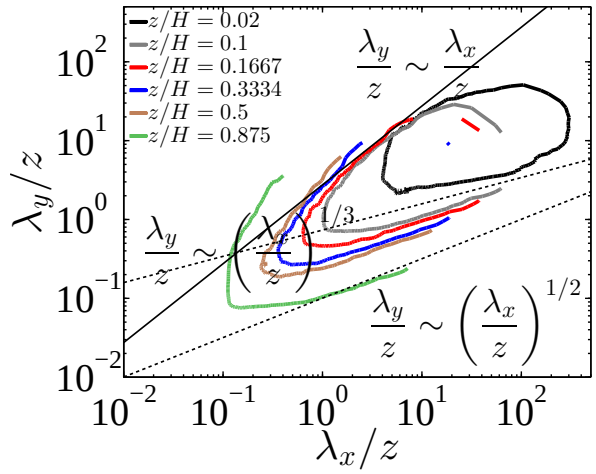

(a)

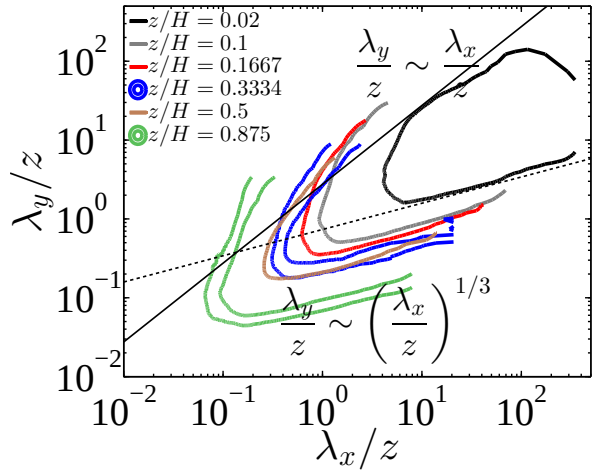

(b)

FIGURE 8: COMPARISON OF 2D PREMULTIPLIED u ENERGY SPECTRA $k_x k_y E_{uu}(k_x, k_y, z)/u_\tau^2$ IN STREAMWISE-SPANWISE WAVE NUMBER SPACE BETWEEN, (A) WITHOUT WIND TURBINES, (B) WITH WIND TURBINES.

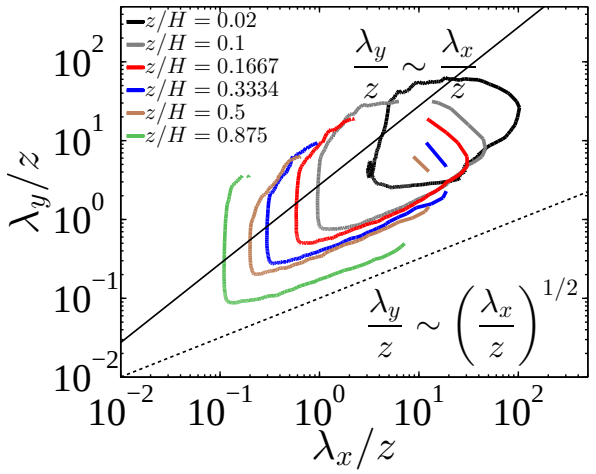

(a)

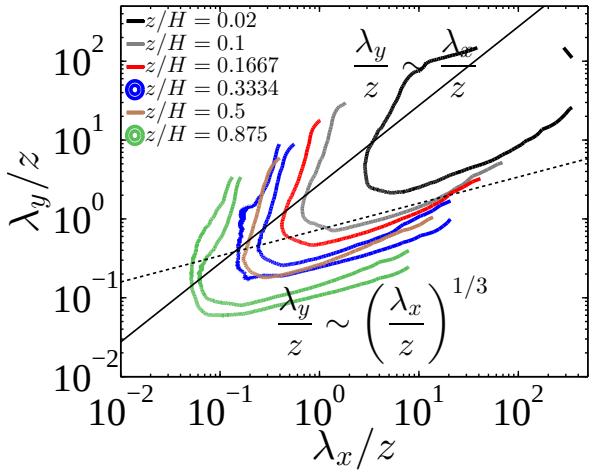

(b)

FIGURE 9: COMPARISON OF 2D PREMULTIPLIED v ENERGY SPECTRA $k_x k_y E_{vv}(k_x, k_y, z)/u_\tau^2$ IN STREAMWISE-SPANWISE WAVE NUMBER SPACE BETWEEN, (A) WITHOUT WIND TURBINES, (B) WITH WIND TURBINES.

near wall attached eddies, e.g., a sweep-ejection pair conditional eddies that constitute important dynamical features of the buffer / log layer. The neutral ABL again shows excellent scaling laws of the 2D u spectra well validated with the theory as well as the past numerical results [18]. Very near to the wall, ($z/H < 0.1$) similarity scaling laws of u spectra (Figure 8a) of "wall-attached eddies" indicate $\lambda_y \sim \lambda_x$ for $\lambda_x \lessapprox 10z$ benchmarked against the wall-bounded DNS [18]. For, $v, w, -\overline{u'w'}$ spectra (respectively for Figures 9a, 10a, 11a) the core of the wall-attached eddies also shows similar trends of $\lambda_y \sim \lambda_x$. Presence of such scaling laws of near-wall attached eddies can also be found in WT arrays (Figure 8b, 9b, 10b, 11b). The larger near-wall eddy sizes for the WT arrays ($u, v, w, -\overline{u'w'}$ spectra), are supposedly bigger than that for neutral ABL, admitting higher magnitudes of λ_x, λ_y. At $z/H = 0.02$ for $k_x k_y E_{uu}$ we obtain the minimum length scales $\lambda_x \sim 4z, \lambda_y \sim 3z$ for both neutral ABL and WT arrays (Figures 8a, 8b) indicating the scale being imposed by $z_{0,lo} = z_0$, the bottom wall roughness. While for neutral ABL, the maximum lengthscale at $z/H = 0.02$ is $\lambda_x \sim 300z, \lambda_y \sim 20z$ corresponding to narrower-longer scale structures ($\lambda_x > \lambda_y$), WT arrays admit much larger maximum length scales (λ_x, λ_y) due to imposing a large eddy size from the "wind turbine array" roughness $z_{0,hi}$.

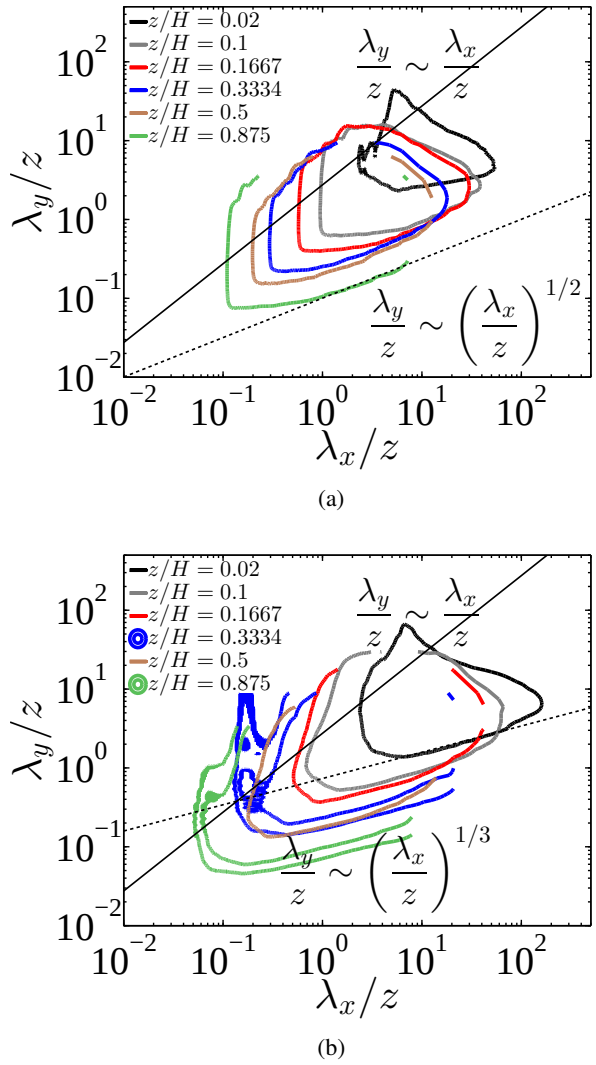

FIGURE 10: COMPARISON OF 2D PREMULTIPLIED w ENERGY SPECTRA $k_x k_y E_{ww}(k_x, k_y, z)/u_\tau^2$ IN STREAMWISE-SPANWISE WAVE NUMBER SPACE BETWEEN, (A) WITHOUT WIND TURBINES, (B) WITH WIND TURBINES.

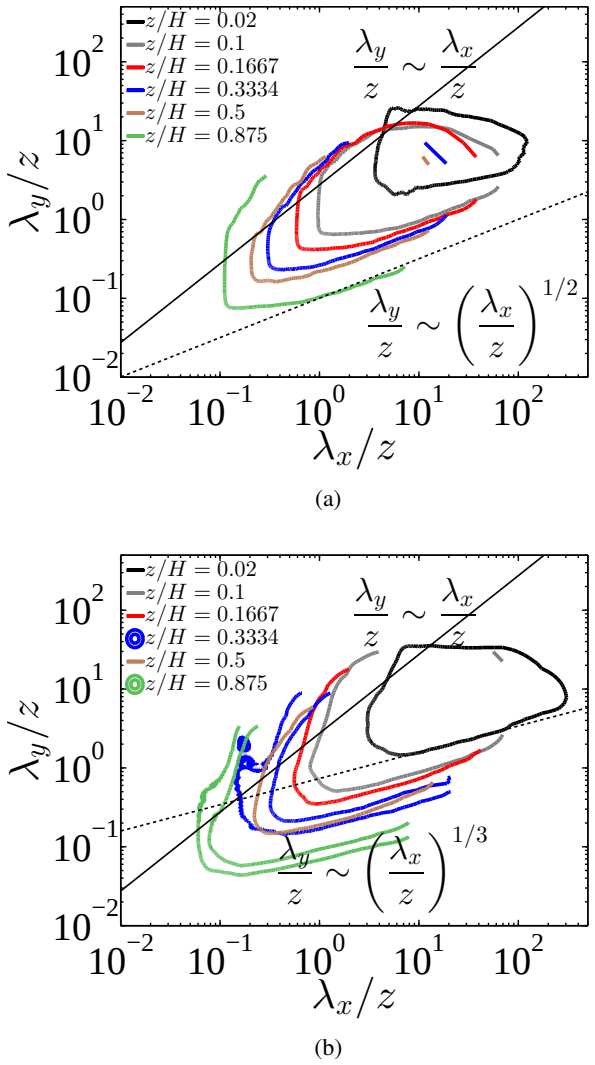

FIGURE 11: COMPARISON OF 2D PREMULTIPLIED uw SHEAR STRESS SPECTRA $k_x k_y \phi_{uw}(k_x, k_y, z)/u_\tau^2$ IN STREAMWISE-SPANWISE WAVE NUMBER SPACE BETWEEN, (A) WITHOUT WIND TURBINES, (B) WITH WIND TURBINES.

The broken region of the u spectra of WT array also indicate that larger structures of the size of LSM's, VLSM's are also present in the near wall region due to the turbine effects which cannot be captured due to the limitations in size of the computational domain. Similar trends of bigger λ_x, λ_y from $v, w, -\overline{u'w'}$ spectra near the wall can also be seen in Figures 9b, 10b, 11b compared to neutral ABL which consistently identifies the effects of wind turbine array as a "roughness element", since the size of the roughness elements does not jeopardize the attached eddy hypothesis, but imposes a minimum length scale on the eddies [7].

Completely different physics are observed between the neutral ABL and the WT array while analysing the rotor-swept area and outer-layer. In the rotor-swept area (hub-height $z/H = 0.333$), we observe conspicuous *spectral-handles* (bimodal characteristics) in the $w, -\overline{u'w'}$ spectra of the WT array. The physical significance of the bimodal behaviour is that new eddy structures are present in WT array compared to an ABL, that are responsible for the "energy injection mechanism". The length scales of these eddies are $\lambda_x \sim 0.05H$ or $0.1D$ conforming to what is seen in the 1D spectra. An interesting observation is that the eddies responsible for the energy injection are wider structures

($\lambda_x < \lambda_y$) possibly due to effects of rotation component in the y direction intercepted by the ABL flow. Both the 1D and 2D spectra indicate that the w component plays a dominant role in the "energy" and "shear-stress" injection at length scales $\sim 0.1D$ corroborating the *downward entraining mechanism* of turbulent shear-stress flux for wind turbine power generation.

Additionally, the long-narrow structures ($\lambda_x > \lambda_y$) in the outer layer of neutral ABL ($u, v, w, -\overline{u'w'}$ spectra) depict a $\lambda_y/z \sim (\lambda_x/z)^{1/2}$ scaling [18]. This clearly indicates the effects of long-time turbulent dissipation on a time-scale t_e. If spanwise diffusion is given as $\lambda_y = (\nu_t t_e)^{1/2}$, with $\nu_t \sim \kappa u_\tau z$ for the logarithmic layer, the bulk flow in the streamwise direction admits $\lambda_x \approx U_s t_e$ with U_s being a characteristic velocity. This gives the square-root scaling for longer-narrower structures ($\lambda_x/\lambda_y \sim 10$) in ABL.

However, in the WT arrays, we observe a new power law scaling $\lambda_y/z \sim (\lambda_x/z)^{1/3}$ for longer-narrower structures in the outer layer which even extends to the near-wall layer as shown by excellent match of $u, w, -\overline{u'w'}$ spectra over roughly a decade of wavelengths $\lambda_x/z \sim 10^0 - 10^1$ at $z/H = 0.02$. The series of turbulent wakes in wind farm creates a streaky flow (spanwise modulation) in the streamwise direction with S being the imposed shear scale (velocity gradient of the spanwise modulation) of the wakes. With $\lambda_x = S\lambda_y t_e$, ($\lambda_y \sim 3D$ or H for spanwise modulation), and assuming the width and the height are the same for cylindrical wakes, the $1/3$ scaling law can be derived from a straightforward algebraic manipulation. Since the wind turbines in the spanwise direction are repeated after every 3D distances, for $\lambda_y \sim 3D$ in the rotor-swept area, the $1/3$ scaling law refers to the dissipation effects imposed by the spanwise shear in the high-speed flow region in between the turbines. The scaling law $\lambda_y/z \sim (\lambda_x/z)^{1/3}$ can also be observed in the near wall narrow structures of the u spectra of WT-array and the neutral ABL due to the presence of similar near wall streaky structures generated from the streamwise rolls [19].

1D premultiplied Spectra

Figure 12 depicts the variation of normalized 1D premultiplied streamwise energy spectra $k_x E_{uu}(k_x, z)/u_\tau^2$ with normalized distance from the wall z/H. The plots and hence the analysis for shear stress spectra is quite similar and hence not reported here. Since the size of the computational domain is not large enough to capture the LSM's and VLSM's [8] in the flow, the neutral ABL flows still predict the **unimodal** characteristic of the z variation of the spectra, representing only the near-wall eddies. For neutral ABL as well as WT array, a linear growth of streamwise length scales $\lambda_x/H \sim O(z/H)$ for a band of energy can be observed at $z/H < 0.1$ depicting the wall-attached eddies [20]. Additionally, in WT-arrays a distinct **bimodal spectra** can be observed due to the presence of wall bounded turbulence production in the log layer as well as production in the rotor swept area due to wind turbines. In the rotor-swept area containing the wake and beyond $z/H \sim 0.1$ we observe strong deviations from the linear growth of the length scales with $\lambda_x/H \sim (z/H)^2$ corresponding to the strong turbulent mixing due to the turbine rotation.

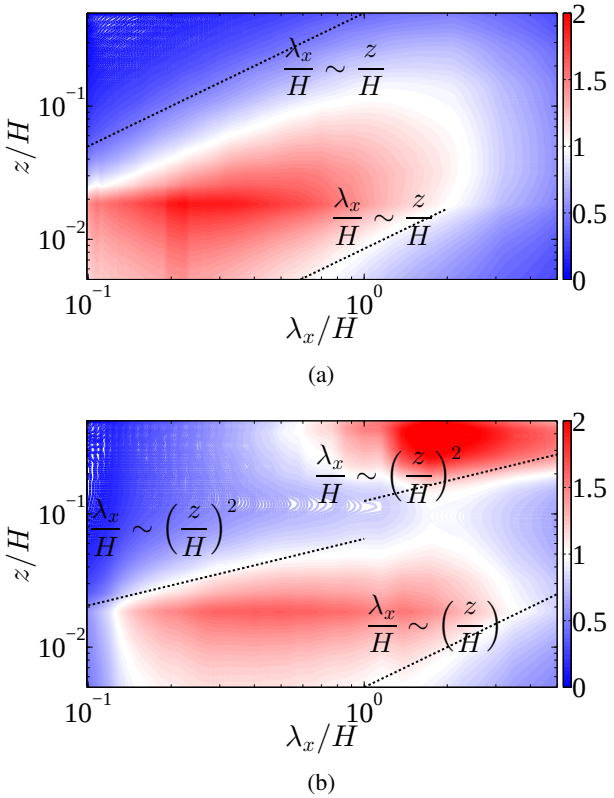

FIGURE 12: VARIATION OF SPANWISE AVERAGED PREMULTIPLIED 1D STREAMWISE ENERGY SPECTRA $k_x E_{uu}(k_x, z)/u_\tau^2$ IN λ_x, z PLANE WITHOUT (A) AND WITH (B) WIND TURBINE ARRAY.

CONCLUSION

In this section we address the answer to the three questions raised in the Introduction section sequentially by summarising the key novel findings in this study.

(a) The 1D spectral analysis reveals that the streamwise length scales $\lambda_x \sim 0.1D$ are dominantly responsible for the power generation from turbulence mainly through the extraction of energy from w component and $-\overline{u'w'}$ (shear stress), in line with the findings of Hamilton et al. [9]. However, much larger scales $\lambda_x \sim 6D$ are also seen to contribute to the power generation in the turbines from u energy.

(b) The "highly correlated" attached eddy layer ($\lambda_y/z \sim \lambda_x/z$) in the near-wall is found to exist even in the presence of turbine arrays. However, streamwise anisotropic long-narrow large scale near wall structures (possibly, LSM's; $\lambda_x/\lambda_y > 10$) in the WT ar-

ray are found to be much *larger* than in neutral ABL. Also, contrary to the near-wall structures, the anisotropic eddies responsible for power generation at hub-height are wider in the spanwise direction ($\lambda_y/\lambda_x > 10$).

(c) We observe a new power law scaling $\lambda_y/z \sim (\lambda_x/z)^{1/3}$ (2D spectra) imposed by the spanwise shear of the turbine wakes (similar to near-wall streaks) in the outer layer which were mostly dominated by dissipative scaling $\lambda_y/z \sim (\lambda_x/z)^{1/2}$ in the neutral ABL. Furthermore, similar to a near-wall linear scaling $\lambda_x/H \sim z/H$ for attached eddies with height, we revive a quadratic scaling $\lambda_x/H \sim (z/H)^2$ corresponding to the turbulent mixing region in the rotor-swept area from the 1D premultiplied spectra.

The knowledge of the length scales of the energy-containing eddies responsible for power production retains its novelty and importance not only for understanding the wind-farm dynamics but can be directly applied in low-order numerics as well as wind plant control. For example, a *reduced order turbulence model* like **RANS** can be designed efficiently with the grid sizes only sufficient to capture the energy containing eddies responsible for power generation and also utilize the information of the *scaling laws* as above in the eddy-viscosity model, which would significantly reduce the computing cost compared to LES yet providing a realistic estimate of the wind-farm power. Also in the present study, we have seen the contribution of *LSM*'s in power generation in the outer layer. Since *LSM*'s are also generated in the near-wall layer due to the wind turbine array possibly due to the "vertical entrainment" of turbulent shear stress, wind turbines with smaller hub-heights and rotor radius can be employed in between the bigger wind turbines for extracting energy from the near-wall *LSM*'s.

ACKNOWLEDGMENT

The authors acknowledge the support of NSF-CBET 13358568 grant and the start-up allocation hours in XSEDE supercomputing cluster for their present work.

REFERENCES

[1] Frandsen, S., Barthelmie, R., Pryor, S., Rathmann, O., Larsen, S., Hojstrup, J., and Thogersen, M., 2006. "Analytical modelling of wind speed deficit in large offshore wind farms". *Wind. Energy.,* ***9***, pp. 39–53.

[2] Calaf, M., Meneveau, C., and Meyers, J., 2010. "Large eddy simulation study of fully developed wind-turbine array boundary layers". *Phys. Fluids.,* ***22***, p. 015110.

[3] Pope, S. B., 2000. *Turbulent Flows*. Cambridge Press.

[4] Reynolds, W. C., 1990. "The potential and limitations of direct and large eddy simulations". In *Lecture Notes in Physics*, Vol. 357. J. L. Lumlery, Ed., Springer-Verlag, Berlin, pp. 313–343.

[5] Porté-Agel, F., Meneveau, C., and Parlange, M. B., 2000. "A scale-dependant dynamics model for large eddy simulation: application to a neutral atmospheric boundary layer". *J. Fluid. Mech.,* ***415***, pp. 261–284.

[6] Townsend, A. A., 1961. "Equilibrium layers and wall turbulence". *J. Fluid. Mech.,* ***11***, pp. 97–120.

[7] Perry, A. E., Henbest, S., and Chong, M. S., 1986. "Theoretical and experimental studies of wall turbulence". *J. Fluid. Mech.,* ***165***, pp. 163–199.

[8] Balakumar, B. J., and Adrian, R. J., 2007. "Large and very-large-scale motions in channel and boundary-layer flows". *Phil. Trans. R. Soc.,* ***365***, pp. 665–681.

[9] Hamilton, N., Kang, H. S., Meneveau, C., and Cal, R. B., 2012. "Statistical analysis of kinetic energy entrainment in a model wind turbine array boundary layer". *J. Renewable and Sustainable Energy,* ***4***, p. 063105.

[10] Cal, R. B., Lebron, J., Kang, H. S., Castillo, L., and Meneveau, C., 2010. "Experimental study of the horizontally averaged flow structure in a model wind-turbine array boundary layer". *J. Renewable and Sustainable Energy,* ***2***, p. 013106.

[11] Sørensen, J. N., and Shen, W. Z., 2002. "Numerical modelling of wind turbine wakes". *J. Fluids Eng.,* ***124***, pp. 393–399.

[12] Fischer, P., Lottes, J., Pointer, D., and Siegel, A., 2008. "Petascale algorithms for reactor hydrodynamics". *J. Phys. Conf. Series,* ***125***, p. 012076.

[13] Mason, P. J., and Thompson, D. J., 1992. "Stochastic backscatter in large-eddy simulations of boundary layers". *J. Fluid. Mech.,* ***242***, pp. 51–78.

[14] Chatterjee, T., and Peet, Y., 2015. Actuator line wind turbine simulations in atmospheric turbulent flows using spectral element method. AIAA paper 2015–0727. 05 - 09 January 2015, Kissimmmee, Florida.

[15] Monin, A. S., and Obukhov, A. M., 1954. "Basic laws of turbulent mixing in the ground layer of the atmosphere". *Trans. Geophys. Inst. Akad. Nauk. USSR,* ***151***, pp. 163–187.

[16] Troldborg, N., 2008. "Actuator line modeling of wind turbine wakes". PhD thesis, Technical University of Denmark.

[17] Brasseur, J. G., and Wei, T., 2010. "Designing large eddy simulation of turbulent boundary layer to capture law-of-wall scaling". *Phys. Fluids,* ***22***, p. 021303.

[18] Alamo, J. D., Jiménez, J., , Zandonade, P., and Moser, R., 2004. "Scaling of the energy spectra of turbulent channels". *J. Fluid. Mech.,* ***500***, pp. 135–144.

[19] Jiménez, J., Alamo, J. D., and Flores, O., 2004. "The large-scale dynamics of near-wall turbulence". *J. Fluid. Mech.,* ***505***, pp. 179–199.

[20] Jiménez, J., 2012. "Cascades in wall bounded turbulence". *Annu. Rev. Fluid. Mech.,* ***44***, pp. 27–45.